Chinese Journal of Natural Medicines

TSZAF monomer combination downregulates the Wnt/β-catenin signaling pathway and inhibits neutrophil recruitment to prevent lung cancer metastasis

Pan Yu, Jialiang Yao, Long Zhang, Yanhong Wang, Xinyi Lu, Jiajun Liu, Zujun Que, Yao Liu, Qian Ba, Jiwei Liu, Yan Wu, Jianhui Tian

Citation: Pan Yu, Jialiang Yao, Long Zhang, Yanhong Wang, Xinyi Lu, Jiajun Liu, Zujun Que, Yao Liu, Qian Ba, Jiwei Liu, Yan Wu, Jianhui Tian, TSZAF monomer combination downregulates the Wnt/β-catenin signaling pathway and inhibits neutrophil recruitment to prevent lung cancer metastasis, Chinese Journal of Natural Medicines, 2025, 23(9), 1069-1079. doi: 10.1016/S1875-5364(25)60973-3.

View online: https://doi.org/10.1016/S1875-5364(25)60973-3

Chinese Journal of Natural Medicines 23 (2025) 1069-1079

Contents lists available at ScienceDirect

Chinese Journal of Natural Medicines

journal homepage: www.cjnmcpu.com/

Original article

TSZAF monomer combination downregulates the Wnt/β-catenin signaling pathway and inhibits neutrophil recruitment to prevent lung cancer metastasis

Pan Yu[a,Δ], Jialiang Yao[a,Δ], Long Zhang[a], Yanhong Wang[a], Xinyi Lu[a], Jiajun Liu[b], Zujun Que[b], Yao Liu[a], Qian Ba[c], Jiwei Liu[d], Yan Wu[d,*], Jianhui Tian[a,b,*]

[a] *Clinical Oncology Center, Shanghai Municipal Hospital of Traditional Chinese Medicine, Shanghai University of Traditional Chinese Medicine, Shanghai 200071, China*
[b] *Institute of Oncology, Shanghai Municipal Hospital of Traditional Chinese Medicine, Shanghai University of Traditional Chinese Medicine, Shanghai 200071, China*
[c] *Science and Technology Innovation Center, Shanghai Municipal Hospital of Traditional Chinese Medicine, Shanghai University of Traditional Chinese Medicine, Shanghai 200071, China*
[d] *Shanghai Mental Health Center, Shanghai Jiao Tong University School of Medicine, Shanghai 200030, China*

ARTICLE INFO

Article history:
Received 23 June 2024
Revised 21 September 2024
Accepted 27 September 2024
Available online 20 September 2025

Keywords:
Circulating tumor cells (CTCs)
Lung cancer
Metastasis
Wnt/β-catenin
Neutrophil
CXCL5

ABSTRACT

Metastasis remains the primary cause of cancer-related mortality worldwide. Circulating tumor cells (CTCs) represent critical targets for metastasis prevention and treatment. Traditional Chinese medicine may prevent lung cancer metastasis through long-term intervention in CTC activity. Tiao-Shen-Zhi-Ai Formular (TSZAF) represents a Chinese medicine compound prescription utilized clinically for lung cancer treatment. This study combined three principal active ingredients from TSZAF into a novel TSZAF monomer combination (TSZAF mc) to investigate its anti-metastatic effects and mechanisms. TSZAF mc demonstrated significant inhibition of proliferation, migration, and invasion in CTC-TJH-01 and LLC cells, while inducing cellular apoptosis *in vitro*. Moreover, TSZAF mc substantially inhibited LLC cell growth and metastasis *in vivo*. Mechanistically, TAZSF mc significantly suppressed the Wnt/β-catenin signaling pathway and CXCL5 expression in lung cancer cells and tissues. Additionally, TAZSF mc notably reduced neutrophil infiltration in metastatic lesions. These findings indicate that TSZAF mc inhibits lung cancer growth and metastasis by suppressing the Wnt/β-catenin signaling pathway and reducing CXCL5 secretion, thereby decreasing neutrophil recruitment and infiltration. TSZAF mc demonstrates potential as an effective therapeutic agent for lung cancer metastasis.

1. Introduction

Lung cancer represents the malignant tumor with the highest incidence and mortality rate among cancer-related deaths globally [1]. In China, lung cancer diagnoses exceeded 800 000 cases in 2022, with annual mortality surpassing 700 000 cases, and these figures continue to increase [2]. Metastasis constitutes a fundamental factor in the high mortality rate among lung cancer patients [3]. Although advances in targeted therapies and immunotherapies have substantially improved survival rates, the 5-year overall survival rate remains under 20% [4]. This limitation primarily stems from most treatments targeting the primary tumor, leaving a significant gap in effective anti-metastatic therapies and clinical models for drug screening.

During tumor progression, cells at the lesion margin undergo epithelial-mesenchymal transformation, entering circulating tumor cells (CTCs) [5]. CTCs demonstrate resistance to blood flow shear stress and evade immune surveillance mechanisms, including natural killer (NK) cells [6, 7]. These cells subsequently disseminate and colonize target organs through vascular extravasation, becoming disseminated tumor cells (DTCs) [8, 9]. CTCs therefore play a crucial role in lung cancer metastasis. Clinical studies indicate that CTCs are detectable in postoperative early-stage lung cancer patients [10], with elevated CTC counts correlating to poorer prognosis [11, 12]. These findings underscore the urgent necessity for developing drugs targeting CTCs to prevent metastasis in postoperative lung cancer patients.

The Wnt signaling pathway demonstrates a strong correlation with tumor cell proliferation, invasion, and metastasis [13–15]. In the off-state of Wnt signaling, β-catenin undergoes phosphorylation for proteasomal degradation. In the on-state, stable β-catenin translocates into the nucleus, where it binds with LET/TCF transcription factors to initiate transcription and translation of downstream target genes, including *c-Myc*, *Cyclin D1*, and *MMP-7*, thereby enhancing the invasive metastatic capacity of tumor cells [16–18]. Consequently, β-catenin serves as a crucial effector molecule in the Wnt signaling pathway [19]. The development of drugs targeting β-catenin and enhancing drug-binding stability may inhibit invasive metastasis of lung cancer [20]. Neutro-

* Corresponding author.
E-mail addresses: drwuyan@163.com (Y. Wu); tjhhawk@shutcm.edu.cn (J. Tian)
Δ These authors contributed equally to this work.

https://doi.org/10.1016/S1875-5364(25)60973-3

phils exhibit dual roles in tumor progression and metastasis [21]. These cells can be influenced by tumors, activating signaling cascades such as JAK/STAT, which suppress the immune system network and facilitate immune evasion by malignant cells [22]. Neutrophil recruitment occurs through chemokines including CXCL5, CXCL1, CXCL2, interleukin 8 (IL-8), and others [23].

The anti-tumor effects of traditional Chinese medicine compounds are characterized by multi-components, multi-pathways and multi-targets [24]. Tiao-Shen-Zhi-Ai Formula (TSZAF) is a traditional Chinese formulation comprising *Zizyphus jujuba*, *Astragalus membranaceus*, *Paris polyphylla* and *Curcuma aromatica*, demonstrating significant clinical efficacy against tumors. TSZAF follows the Jun-Chen-Zuo-Shi principle, representing Monarch-Minister-Assistant-Facilitating assistant. *Zizyphus jujuba* derived from the Suan-Zao-Ren decoction in *Huangdi Neijing* (*Huangdi's internal classic*), nourishes blood and calms the mind, with Jujuboside A (JBA) as its active ingredient. *Astragalus membranaceus* (Fisch.) tonifies *yang* and supplements *qi*, regulating immunity to exert anti-tumor efficacy, with Astragaloside Ⅳ (AS Ⅳ) as its effective component. *Paris polyphylla* clears heat and removes toxins, demonstrating significant anti-tumor efficacy in recent studies [25], with Paris saponin Ⅶ (PS Ⅶ) as its representative compound. *Curcuma aromatica* regulates *qi* and relieves stagnation, with curcumin (CCM) as its typical component. While TSZAF has been granted a patent (ZL 202210718678.8), its anti-tumor mechanism remains to be elucidated.

This study examines the main effective active ingredients from TSZAF, combined as TAZAF mc (PS Ⅶ, AS Ⅳ and JBA), to investigate their effects on lung cancer growth and metastasis and elucidate the anti-metastasis mechanism.

2. Materials and methods

2.1. Chemicals and reagents

PS Ⅶ (CAS No. 68124-04-9; PubChem CID: 176233; molecular formula: $C_{51}H_{82}O_{21}$; molecular weight: 1031.2; high performance liquid chromatography (HPLC) ≥ 98%), AS Ⅳ (CAS No. 84687-43-4; PubChem CID: 13943297; molecular formula: $C_{41}H_{68}O_{14}$; molecular weight: 784.97; HPLC ≥ 98%), JBA (CAS No. 55466-04-1; PubChem CID: 51346169; molecular formula: $C_{58}H_{94}O_{26}$; molecular weight: 1207.6; HPLC ≥ 98%), CCM (CAS No. 458-37-7; PubChem CID: 969516; molecular formula: $C_{21}H_{20}O_6$; molecular weight: 368.38; HPLC ≥ 98.5%) were obtained from Push Bio-Technology Co., Ltd. (Chengdu, China). The chemicals were dissolved in DMSO and stored at −20 °C. Prior to each experiment, the chemicals were diluted with medium to achieve a DMSO concentration below 0.1%. Cell counting kit-8 (CCK-8) (#CK-04) was acquired from Dojindo (Shanghai, China). Fluorescein isothiocyanate (FITC) Annexin V apoptosis detection kit (#556547) and PI/RNase staining buffer (#550825) were procured from BD Pharmingen (CA, USA). Ribonucleic acid (RNA) extraction kit (#RR430S) and PrimeScript™ RT Master Mix (RRA036) were obtained from TaKaRa (Beijing, China). Antibodies specific for MMP-2 (#AF5330), MMP-9 (#AF5228), E-Cadherin (#BF0219), *β*-catenin (#AF6266), WNT-3α (#DF6113), MMP-7 (#AF0218), CXCL1 (#AF5403), CXCL5 (#DF9919), Ki-67 (#AF0198), c-caspase 3 (#AF7022), and *β*-actin (#T0022), were acquired from Affinity Bioscience. Antibodies specific for p-*β*-catenin (#4176T), IL-8 (#94407), goat anti-mouse IgG-HRP (#56970), donkey anti-rabbit IgG-HRP (#7074), and Ly-6G (FITC-Conjugate) (#88876S) were obtained from Cell Signaling Technology (Danvers, MA, USA). Antibody specific for c-Myc (#GTX103436) was procured from GeneTex (San Antonio, Texas, USA). Antibody specific for Cyclin D1 (60186-1-Ig) was obtained from Proteintech (Wuhan, China). Antibody specific for CD16/CD32 (553142) was acquired from BD (CA, USA), CD11b-APC/Cy7 (#101262) and Ly6G-FITC (#127068) were obtained from Biolegend (Beijing, China).

2.2. Cell culture

Human circulating lung cancer cell line CTC-TJH-01 was established by our team [26]. LLC cells were obtained from the Cell Bank of the Chinese Academy of Science (Shanghai, China). CTC-TJH-01 cells were maintained in F12K medium (basal media, Shanghai, China). LLC cells were maintained in DMEM (Corning Cellgro, USA), supplemented with 10% (*V*/*V*) fetal bovine serum (Biological Industries) and 1% (*V*/*V*) penicillin-streptomycin. All cells were incubated in a humidified atmosphere with 5% CO_2 at 37 °C.

2.3. Cell viability assay

CTC-TJH-01 and LLC cells were seeded into 96-well plates and preincubated for 24 h at 37 °C with 5% CO_2. Subsequently, cells were incubated with fresh medium containing TSZAF mc at specific concentrations. For cell viability assessment, the cell plate was incubated with CCK-8 for 2 h after 24 and 48 h. The optical density (OD) was measured at 450 nm using the UV–vis cell plate reader and normalized against control cells without TSZAF monomer incubation.

2.4. Colony forming assay

CTC-TJH-01 and LLC cells were seeded into 6-well plates (600 cells/well) and treated with TSZAF mc at different concentrations for 10 d. The cells were fixed with 4% paraformaldehyde and stained with Giemsa, followed by phosphate-buffered saline (PBS) washing twice. Images were captured after staining and the number of cell clones was quantified.

2.5. Flow cytometry assay

For cell cycle analysis, CTC-TJH-01 and LLC cells were treated with varying concentrations of TSZAF mc for 24 h. The cells were collected, washed once with PBS, and resuspended in 1 mL precooled 70% ethanol. After fixation at 4 °C for 2 h, cells were washed once with PBS, stained with PI/RNase at room temperature for 15 min, and analyzed using CytoFLEX (BA11101, Beckman) within 1 h.

For the cell apoptosis assay, CTC-TJH-01 and LLC cells were treated with varying concentrations of TSZAF mc for 24 h. The cells were collected, washed twice with precooled PBS, and resuspended in 300 μL binding buffer containing 5 μL Annexin V-FITC and 5 μL PI for 30 min. Analysis was performed using CytoFLEX within 1 h.

2.6. Transwell migration and invasion assay

The migration and invasion capabilities of tumor cells (CTC-TJH-01 and LLC) were evaluated through a Transwell assay. CTC-TJH-01 (8×10^4) and LLC (1.2×10^5) cells in 500 μL medium without fetal bovine serum (FBS) were placed in the transwell upper chamber, while 750 μL medium containing 20% FBS was added to the lower chamber. For the invasion assay, matrigel was pre-coated in the upper chambers. Following TSZAF mc treatment for 18 h, remaining cells in the upper chamber were removed, fixed with 4% paraformaldehyde for 30 min, and stained with crystal violet for 15 min. After washing twice with double distilled water and drying, images of five random fields were captured using a microscope (Nikon), and migrated and invaded cells were quantified.

2.7. Animal experiment

Five-week-old male C57BL/6J mice were utilized for the mouse models. The animals were maintained under specific pathogen-free (SPF) laboratory conditions in the Animal Laboratory Center. All procedures received approval from the Animal Research Committee of Shanghai Municipal Hospital of Traditional Chinese Medicine, Shanghai University of Traditional Chinese Medicine (SYXK (Shanghai) 2021038). Following one week of adaptive breeding, mice were randomly assigned to two groups: (1) Control group (Control, n = 8), (2) TSZAF mc group (TSZAF mc, n = 8), and received either subcutaneous or tail injection with 5×10^5 LLC cells. The TSZAF mc groups received TSZAF mc (PS Ⅶ (2.5 mg·kg^{-1}), AS Ⅳ (2.5 mg·kg^{-1}), JBA (2.5 mg·kg^{-1}) in 0.2 mL physiological saline with 25% PEG300 thrice weekly, while Control groups received equivalent physiological saline. After 4 weeks, the mice were sacrificed, and tumors or lungs were extracted for further analysis.

2.8. Immunohistochemical (IHC)

The paraffin-embedded tissue specimens underwent sectioning, antigenic repair, and bovine serum albumin (BSA) blocking before incubation with Ki-67, c-caspase 3, *β*-catenin and CXCL5 antibodies at 4 °C overnight. Following secondary antibody incubation, specimens were developed with DAB, counterstained with hematoxylin, and sealed with neutral gum. The sections were examined under a microscope (Leica Biosystems, Wetzlar, Germany), and images were captured and analyzed using Fuji ImageJ software.

2.9. RNA-Sequencing (Seq) analysis

Total RNA from CTC-TJH-01 cells (Control group, n = 3, and TSZAF mc group, n = 3) was extracted using Trizol. The RNA underwent electrophoretic QC and quantitative QC for library construction before analysis on an Illumina sequencing platform. Sequencing was performed using PE150 by Synthesis (SBS, Sequencing by Synthesis). Genome mapping was conducted using HISAT2 software. RNA quantification of comparative data utilized htseq-count software. Expression counts and FPKM matrices obtained through the R package edgeR were used for expression-based differential and significance calculations. Differential messenger RNAs (mRNAs) were visualized using volcano plots. Clustering heatmap visualization was performed for differential mRNA FPKM values. Gene Ontology (GO) & Kyoto Encyclopedia of Genes and Genomes (KEGG) pathway analysis of differential mRNA genes was conducted using the R package.

2.10. Real-time polymerase chain reaction (RT-PCR)

Total RNA was extracted using an RNA extraction kit following the standard protocol. mRNA was reverse transcribed into cDNA using PrimeScript™ RT Master Mix kit. RT-PCR was performed using TB Green Fast Qpcr Mix kit on QuantStudio Dx. Target gene mRNA levels were calculated and normalized using the $2^{-\Delta\Delta CT}$ method. Primer sequences are listed in Table S1.

2.11. Western blotting (WB)

Total protein from CTC-TJH-01 cells treated with varying concentrations of TSZAF mc was extracted using RIPA buffer. Protein concentrations of cell lysates were determined using a BCA assay kit. Subsequently, 30 μg of proteins were loaded onto 10%–15% SDS-PAGE gels, electrophoresed, and transferred to PVDF membranes. The membranes were blocked with 5% fat-free milk in Tris-buffered saline-Tween 20 (TBST) for 1 h at room temperature and incubated with primary antibodies (MMP-2, MMP-9, *E*-cadherin, *β*-catenin, phosphorylation-*β*-catenin, Wnt-3α, c-Myc, Cyclin D1, MMP-7, CXCL1, CXCL5, CXLC8 and *β*-actin) overnight at 4 °C. The membranes underwent four washing cycles (5 min each) with TBST and were incubated with secondary antibodies for 1 h at room temperature, followed by additional TBST washing. The blot images were acquired using an ECL kit (Bio-Rad). Protein density was measured and normalized against *β*-actin using ImageJ software (National Institutes of Health, USA).

2.12. Neutrophil recruitment assay

Mouse spleen immune cells were dissociated into single cells using gentleMACS™ Dissociator (Miltenyi, German). Red cells were eliminated with red cells lysate (Biosharp) and washed twice with PBS. The remaining cells were transferred to the transwell upper chamber for co-cultivation with LLC cells previously treated with TSZAF for 24 h. After 4 h, cells in the lower chamber were collected, blocked with CD16/CD32 for 10 min, then incubated with CD11b-APC/Cy7 and Ly6G-PE antibodies at room temperature under light protection for 15 min. Following two PBS washes, the cells were analyzed using CytoFLEX. All data were processed using FlowJo software (10.4.0, USA).

2.13. Immunofluorescence (IF)

Paraffin-embedded tissue specimens were sectioned, antigenically repaired, blocked with BSA, and incubated with Ly6G and IL-8 antibodies at 4 °C overnight. The specimens were then incubated with a fluorescent secondary antibody and treated with DAPI under light protection. Following decolorization and washing, the specimens were sealed with anti-fluorescence quenching agent. The sections were examined under a fluorescence microscope (Leica Biosystems, Wetzlar, Germany), and images were captured.

2.14. Statistical analysis

All experiments were performed in triplicate (n = 3). The data are expressed as the mean ± SD. Data between two independent groups were compared by Student's t-test, and multiple groups were assessed by one-way ANOVA analysis, with the *LSD-t*-test used for between-group comparisons. $P < 0.05$ was defined as statistically significant. All statistical analyses were performed using GraphPad Prism 8.0.2 (GraphPad) Prism 8.0.2 (GraphPad, SanDiego, CA).

3. Results

3.1. TSZAF mc inhibited the proliferation of CTC-TJH-01 and LLC cells in vitro

To elucidate the anti-tumor effects of components in TSZAF, the effects of four main monomers on the proliferation of CTC-TJH-01 and LLC cells were measured using CCK-8 assay (Fig. S1A). Following traditional Chinese Medicine principles, *Zizyphus jujuba* serves as the monarch medicine, *Paris polyphylla* and *Astragalus membranaceus* function as minister medicines, and *Curcuma aromatica* acts as the assistant medicine. Given that *Curcuma aromatica* and *Zizyphus jujuba* exhibit similar effects, the monomers were combined at equivalent concentrations, creating two combinations differentiated by the presence or absence of CCM. No significant difference in anti-tumor proliferation effects was observed between these combinations (Fig. S1B).

PS Ⅶ, AS Ⅳ and JBA were combined in a 1∶1∶1 ratio to create TSZAF mc. Among these compounds, PS VII demonstrated

proliferation inhibitory properties (Fig. S1A), while AS Ⅳ and JBA potentially modulate immunity and endocrine function. The TSZAF mc concentration was determined based on PS VII levels. The combination of these three monomers demonstrated inhibitory effects on CTC-TJH-01 and LLC cell proliferation (Fig. 1A). Concentrations of 0.5 μmol·L^{-1} and 1.0 μmol·L^{-1} were selected for low and high-concentration groups, respectively. Colony formation assays further validated TSZAF mc's inhibitory effect on CTC-TJH-01 and LLC cells, with significant reductions in clone numbers following treatment (Fig. 1B). Treatment with 1.0 μmol·L^{-1} TSZAF mc induced G1 phase cell cycle arrest (Fig. 1C) and apoptosis in both cell lines (Fig. 1D). These results demonstrate that TSZAF mc effectively inhibited CTC-TJH-01 and LLC cell proliferation.

3.2. TSZAF mc inhibited the growth of LLC cells in vivo

To evaluate TSZAF mc's effects on tumor growth *in vivo*, a subcutaneous tumor model was established in C57BL/6J mice. Following 22 days of TSZAF mc administration, significant reductions in tumor weight and volume were observed (Figs. 2A–2C), while body weight remained consistent between groups (Fig. 2D). IHC staining of tumor tissue for Ki-67 and c-caspase 3 was performed to investigate the mechanism of TSZAF mc's anti-proliferative and tumor-suppressive effects. The results revealed significantly decreased Ki-67 expression and positive cell ratio after TSZAF mc treatment, accompanied by notably increased c-caspase 3 expression Fig. 2E.

3.3. TSZAF mc inhibited the migration and invasion of CTC-TJH-01 and LLC cells

Migration and invasion assays were conducted to evaluate the effect of TSZAF mc on the metastatic capacity of CTC-TJH-01 and LLC cells. As illustrated in Figs. 3A and 3B, TSZAF mc demonstrated significant concentration-dependent inhibition of migration and invasion in both CTC-TJH-01 and LLC cells. Additionally, we examined the protein expression of MMP-2 and MMP-9, which are essential for cell migration and invasion. Fig. 3C demonstrated that TSZAF mc treatment notably decreased the expression of MMP-2 and MMP-9 protein levels in both CTC-TJH-01 and LLC cells. These findings collectively demonstrated that TSZAF mc inhibited lung cancer cell metastasis *in vitro*.

3.4. TSZAF mc inhibited the metastasis of lung cancer in vivo

To investigate the anti-metastatic effect of TSZAF mc, a lung cancer metastasis model was established in C57BL/6J mice through tail injection of LLC cells. The TSZAF mc treatment group exhibited significantly fewer metastatic nodules on the lung surface compared to the control group (Figs. 4A and 4B), while body weights remained comparable between groups (Fig. 4C). HE staining of the lungs revealed a significant reduction in metastatic foci number and lung metastatic load (calculated as metastasis

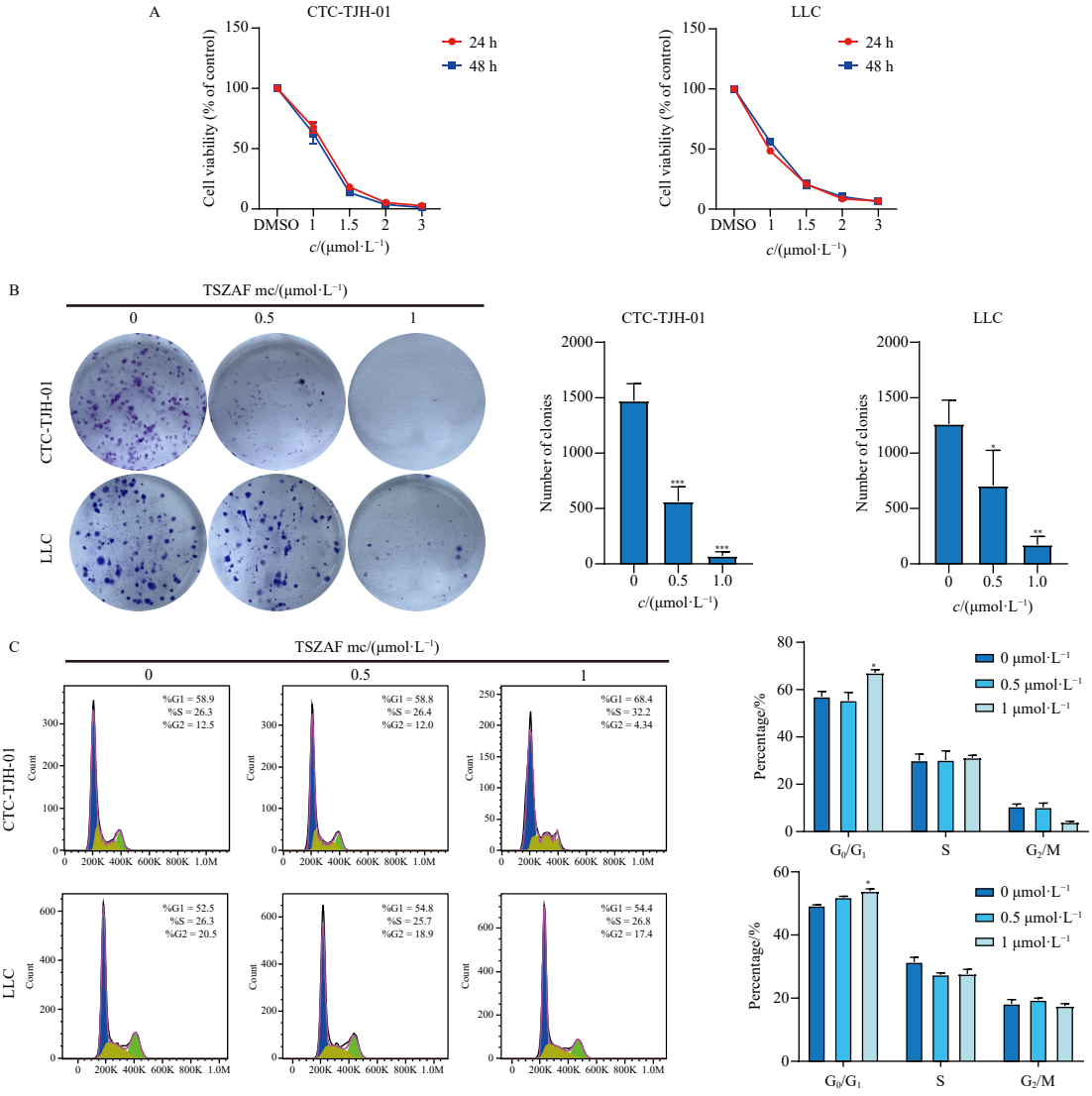

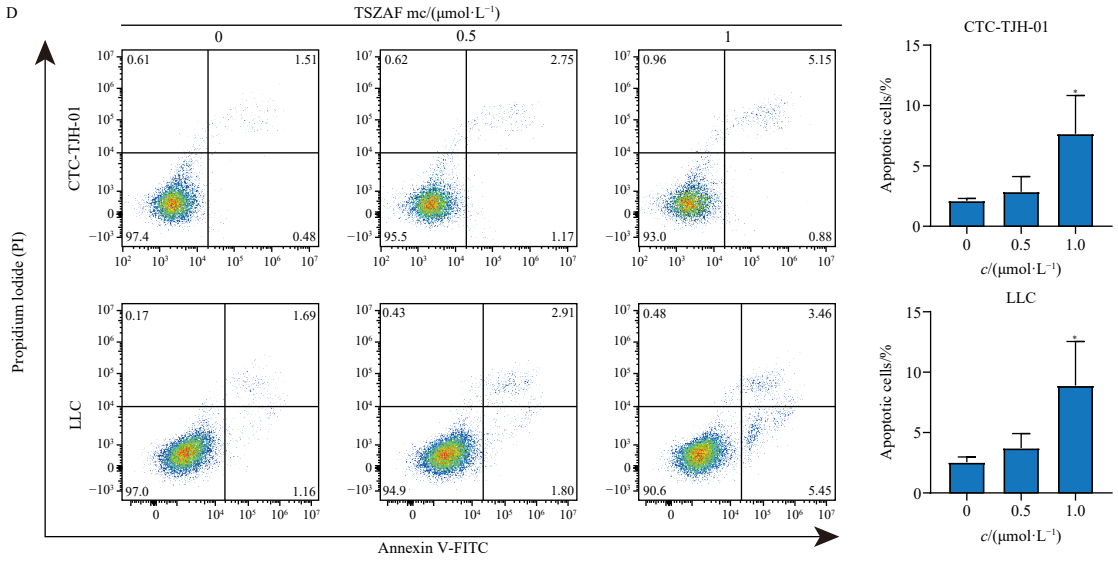

Fig. 1 TSZAF mc inhibited the proliferation of lung cancer cells *in vitro*. (A) CTC-TJH-01 and LLC cells were treated with TSZAF mc (DMSO, 1, 1.5, 2, 3 μmol·L^{-1}) for 24 or 48 h. The CCK-8 assay was used to evaluate the cell viability. (B) Clone formation ability of CTC-TJH-01 and LLC cells after treatment with TSZAF mc (0, 0.5, 1 μmol·L^{-1}). (C) CTC-TJH-01 and LLC cells were treated with TSZAF mc (0, 0.5, 1 μmol·L^{-1}) for 24 h, flow cytometry was used to determine the cell cycle. (D) Cell apoptosis. Each bar represents the mean ± SD of the three separate experiments. $^{*}P < 0.05$, $^{**}P < 0.01$, $^{***}P < 0.001$ *vs* the control group.

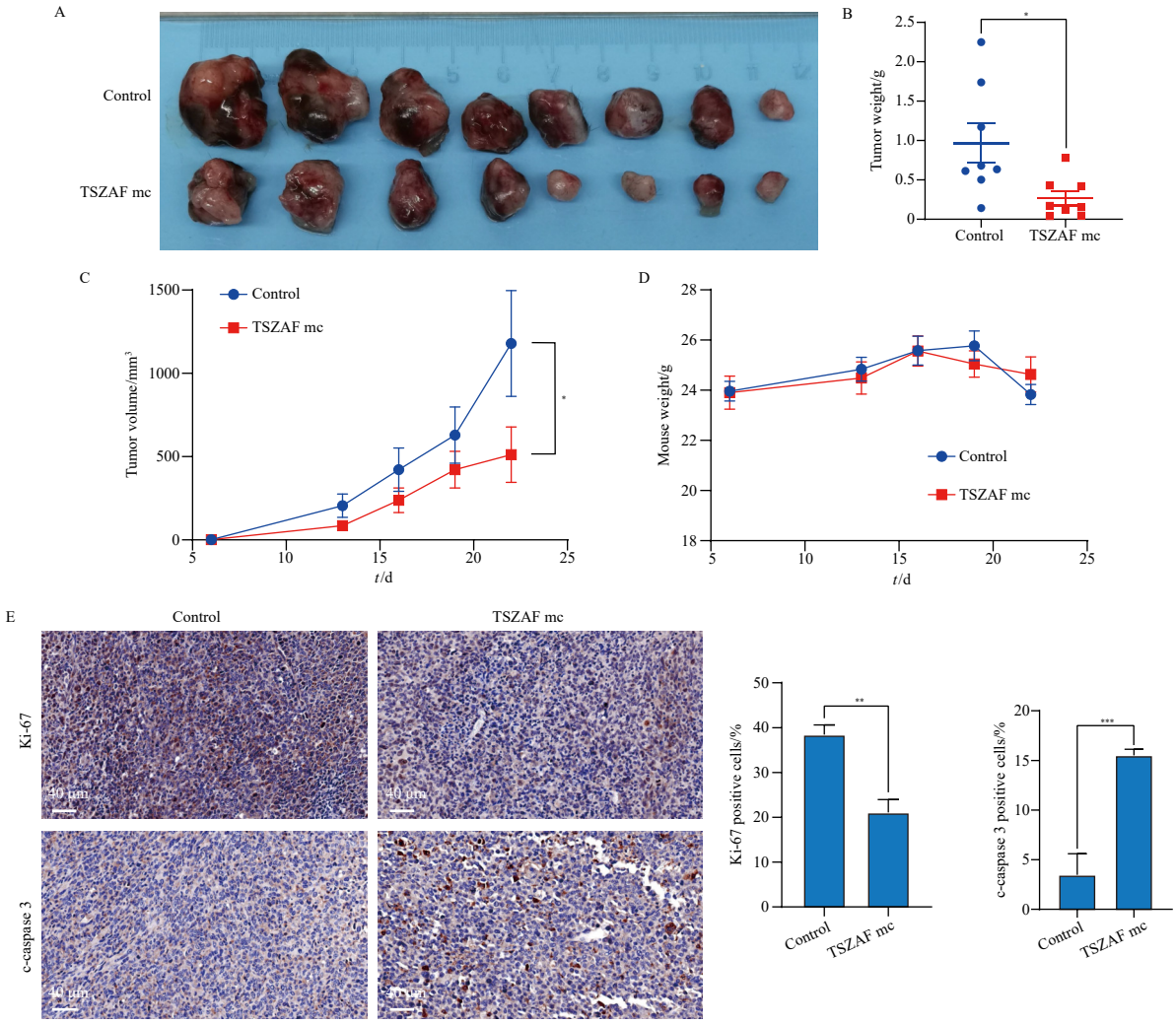

Fig. 2 TSZAF mc inhibited the growth of tumors by suppressing proliferation and inducing apoptosis in *vivo*. C57BL/6J mice were injected subcutaneously with LLC cells, and TSZAF mc was injected intraperitoneally three times a week. (A) An image of tumors in each group on day 22 after injection of tumor cells. (B) Weight and (C) volume of tumors. (D) Weight of mice in the two groups. (E) IHC staining and the number of positive Ki-67 and c-caspase 3 cells in tumor tissue. Scale bar 40 μm. Each bar represents the mean ± SD (n = 8). $^{*}P < 0.05$, $^{**}P < 0.01$, $^{***}P < 0.001$ *vs* the control group.

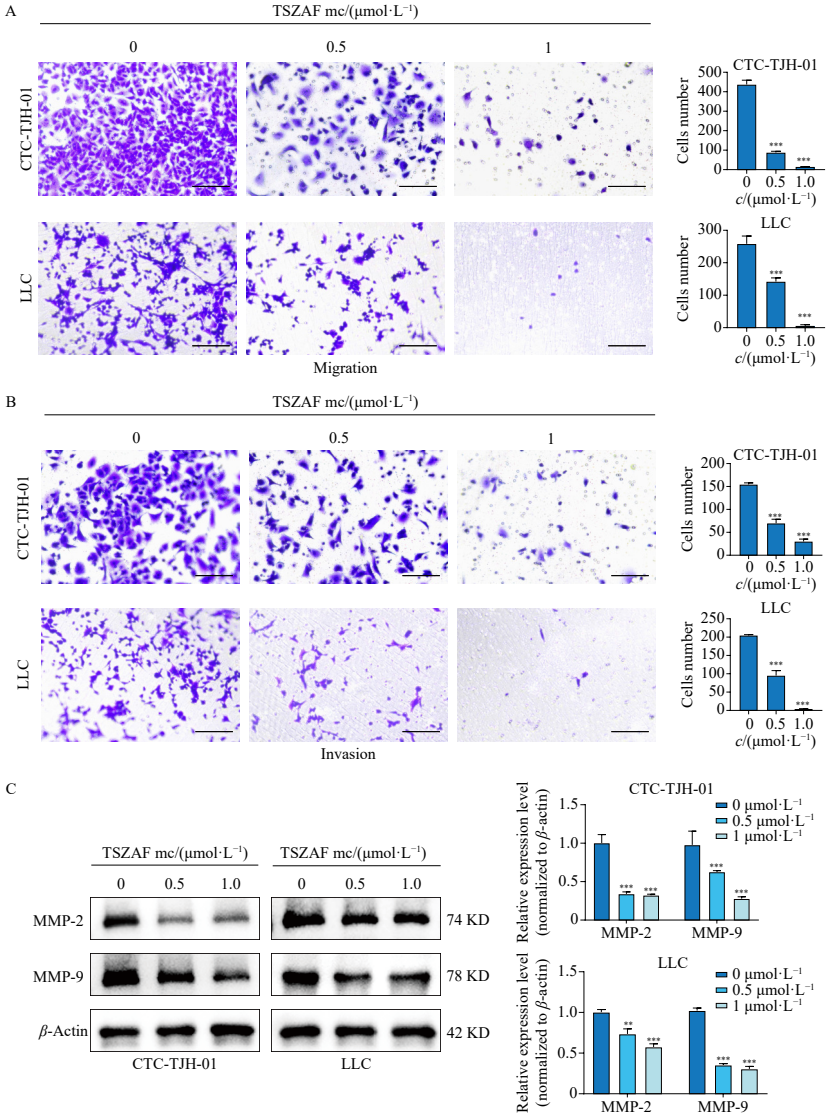

Fig. 3 TSZAF mc inhibited the migration (A) and invasion (B) of lung cancer cells. CTC-TJH-01 and LLC cells were treated with the indicated concentrations (0, 0.5, 1 μmol·L^{-1}) of TSZAF mc for 18 h, then transwell assays were used with and without Matrigel, images were taken by a microscope after staining with crystal violet. (C) The CTC-TJH-01 and LLC cells were exposed to TSZAF mc (0, 0.5, 1 μmol·L^{-1}) for 24 h, the expression of MMP-2 and MMP-9 was detected by WB. *β*-Actin was used as an internal standard. Scale bar 100 μm. Each bar represents the mean ± SD of the three separate experiments. $^{*}P < 0.05$, $^{**}P < 0.01$, $^{***}P < 0.001$ *vs* the control group.

index = tumor area/lung area × 100%) following TSZAF mc treatment (Fig. 4D). IHC staining of lungs for Ki-67 and c-caspase 3 was performed. As shown in Fig. 4E, TSZAF mc treatment resulted in significantly decreased Ki-67 expression and Ki-67 positive cell ratio, while c-caspase 3 expression increased. These results demonstrate that TSZAF mc effectively inhibited lung metastasis formation in mice.

3.5. RNA-Seq analysis of CTC-TJH-01 treated with TSZAF mc

To elucidate the anti-tumor mechanism of TSZAF mc, transcriptome sequencing was performed on CTC cells treated with TSZAF mc for 24 h. As illustrated in Fig. 5A, the heatmap displays upregulated genes in red and downregulated genes in blue. Analysis of differentially expressed genes (fold change > 2) revealed that 78 genes were significantly downregulated and 161 genes were significantly upregulated in TSZAF mc-treated CTC-TJH-01 cells compared to the control group (Fig. 5B). GO and KEGG pathway analyses of the significant genes demonstrated that CDH1 (*E*-cadherin) was significantly upregulated, and the Wnt signaling pathway was enriched (Figs. 5C and 5D). Additionally, the IL-17 signaling pathway (Figs. 5E and 5F) was enriched, while CXCL1, CXCL5, and IL-8, which are closely associated with neutrophil recruitment, were significantly downregulated. These findings suggest that TSZAF mc inhibits lung cancer progression and metastasis through modulation of the Wnt signaling pathway and regulation of neutrophil recruitment.

3.6. TSZAF mc inhibited the Wnt/β-catenin signaling pathway in CTC-TJH-01 and LLC cells

To investigate the mechanism of TSZAF mc on CTC-TJH-01 and LLC cells, the mRNA expression levels in the Wnt/*β*-catenin signaling pathway of CTC-TJH-01 cells were examined. TSZAF mc significantly enhanced the mRNA expression of *E-cadherin* while reducing the expression of *β-catenin*, *APC*, *Wnt-3α*, *c-Myc*, *Cyclin D1* and *MMP-7* (Fig. 6A). Protein expression analysis of the Wnt/*β*-catenin signaling pathway in CTC-TJH-01 and LLC cells by WB demonstrated results consistent with the mRNA findings. Treatment with 1.0 μmol·L^{-1} TSZAF mc led to significant upregulation of E-cadherin and p-*β*-catenin expression, while downregulating *β*-catenin, Wnt-3α, c-Myc, Cyclin D1, and MMP-7 expression (Figs. 6B and 6C). Furthermore, analysis of *β*-catenin protein expression in lung metastases of mice revealed a marked reduction following TSZAF mc treatment (Fig. 6D). These results indicate that TSZAF mc inhibits proliferation through downregulation of

the Wnt/β-catenin signaling pathway.

3.7. TSZAF reduced the neutrophil recruitment by decreasing CXCL5 secretion in lung cancer metastases

Neutrophils play a crucial role in tumor progression and metastases, and evidence suggests that TSZAF mc may reduce neutrophil recruitment through inhibition of chemokine secretion. RT-PCR was employed to detect the mRNA expression of *CXCL1*, *CXCL5* and *IL-8* in CTC-TJH-01 cells treated with TSZAF mc. Additionally, the protein expression of the corresponding chemokines in CTC-TJH-01 and LLC cells was analyzed using WB assay. As demonstrated in Figs. 7A and 7B, the mRNA and protein levels of these three chemokines decreased after TSZAF mc treatment. To evaluate the effect of TSZAF mc on neutrophil recruitment by LLC cells, a recruitment assay revealed a significant reduction in the proportion of neutrophils recruited by LLC cells treated with TSZAF mc (Fig. 7C). IF staining was conducted to detect neutrophil infiltration within lung metastases. As illustrated in Fig. 7D, the expression of Ly6G, a neutrophil marker, significantly decreased following TSZAF mc treatment. Furthermore, IHC results demonstrated significantly reduced CXCL5 expression in the lung metastases of the TSZAF mc group. These findings indicate that TSZAF mc inhibits lung metastasis by reducing neutrophil recruitment through decreased CXCL5 secretion from lung cancer cells.

4. Discussion

Prevention of metastasis represents a critical therapeutic strategy for improving long-term survival in lung cancer patients [27]. However, clinically proven drugs for managing lung cancer metastases remain limited [28]. CTCs circulate in the peripheral blood of lung cancer patients preoperatively or may disseminate in a dormant state to target organs, potentially developing into metastases at a later time [5, 29, 30]. Consequently, developing new anti-metastatic drugs based on CTC cell lines is essential. Our research group previously established a lung cancer CTC line named CTC-TJH-01 for screening effective drugs against lung cancer metastasis [26, 31]. This study investigated the anti-metastatic mechanism of TSZAF mc using CTC-TJH-01 cells and a mouse model of lung metastasis.

TSZAF demonstrates significant anti-tumor efficacy, though its mechanism remains incompletely understood. Given that Chinese medicine prescriptions contain multiple herbal components, making it challenging to fully elucidate their mechanisms within a brief period, we selected three representative monomers for investigation. Previous research indicates that PS Ⅶ, AS IV and JBA exhibit anti-tumor effects through direct or indirect mechanisms. PS Ⅶ inhibited migration and invasion of A549 cells by reducing MMP2 and MMP9 activities through TIMP1/2 up-regulation [32]. Additionally, PS Ⅶ induced autophagy in H460 and PC9 cells by activating adenosine 5'-monophosphate-activated protein kinase (AMPK) and inhibiting mTOR signaling [33]. AS-IV suppressed migration and invasion of A549 cells through the PKC-α-ERK1/2-NF-κB pathway [34]. Furthermore, AS-IV inhibited lung cancer progression and metastasis by modulating macrophage polarization through AMPK signaling [35]. JBA, an agonist of FAT atypical cadherin 4, inhibited proliferation of A549, H1299, and H1975 through HIPPO signaling activation and YAP nuclear translocation inhibition [36]. However, these studies primarily focus on primary tumors, with limited research addressing lung

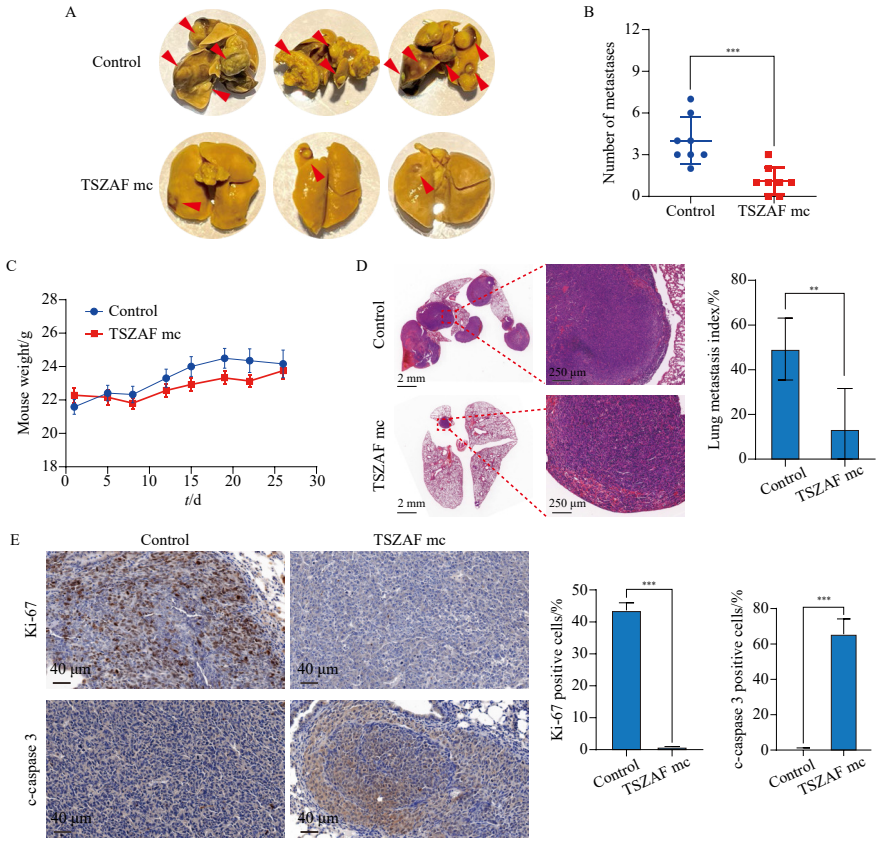

Fig. 4 TSZAF mc inhibited the lung metastasis of tumors by suppressing proliferation and inducing apoptosis in *vivo*. C57BL/6J mice were injected intravenously through tail vein with LLC cells, and TSZAF mc was injected intraperitoneally three times a week. (A) An image of lungs in each group on day 28 after injection of tumor cells. (B) Number of metastatic nodules on the surface of the lungs. (C) Weight of mice in the two groups. (D) Representative HE staining images of lungs. The scale bars indicate 2 mm, 250 μm and 20 μm for 0.5 × , 4 × and 50 × . Index of lung metastasis (calculated as tumor aera/lung aera × 100%) in the two groups. (E) IHC staining and the number of positive Ki-67 and c-caspase 3 cells in tumor tissues. Scale bar 40 μm. Each bar represents the mean ± SD (n = 8). $^{*}P < 0.05$, $^{**}P < 0.01$, $^{***}P < 0.001$ *vs* the control group.

cancer metastases and CTCs. Our previous research demonstrated that Jinfukang, a traditional Chinese medicine prescription, induced DNA damage and apoptosis in CTC-TJH-01 cells and recruited NK cells to inhibit lung cancer metastasis [37–39].

This study demonstrated that TSZAF mc significantly inhibited the invasive migration capability of CTC-TJH-01 cells through the Wnt/β-catenin signaling pathway. The Wnt/β-catenin pathway is implicated in the proliferation, migration, invasion, and epithelial-mesenchymal transition of lung cancer cells [40]. This pathway exhibits potential connections to several other pathways and serves a crucial function in lung cancer development and progression [18, 41]. The abnormal reactivation of the Wnt/β-catenin signaling pathway facilitates the progression of various cancers, including triple-negative breast cancer, intrahepatic cholangiocarcinoma, colorectal cancer, and prostate cancer [14, 15, 42, 43]. The Wnt/β-catenin pathway has also been linked to chemoresistance induction, immune editing, and resistance to immune checkpoint inhibitors [44, 45].

Furthermore, TSZAF mc demonstrated the ability to reduce neutrophil infiltration in the metastatic foci of a lung cancer metastasis mice model. Recent research has extensively documented the roles of neutrophils in tumor metastasis. Peripheral blood neutrophils can adhere to CTCs, forming CTC-neutrophil clusters that protect CTCs from blood flow shear forces and immune surveillance, thereby facilitating efficient CTC spread and metastasis [46]. The abundance of neutrophil infiltration in solid tu-

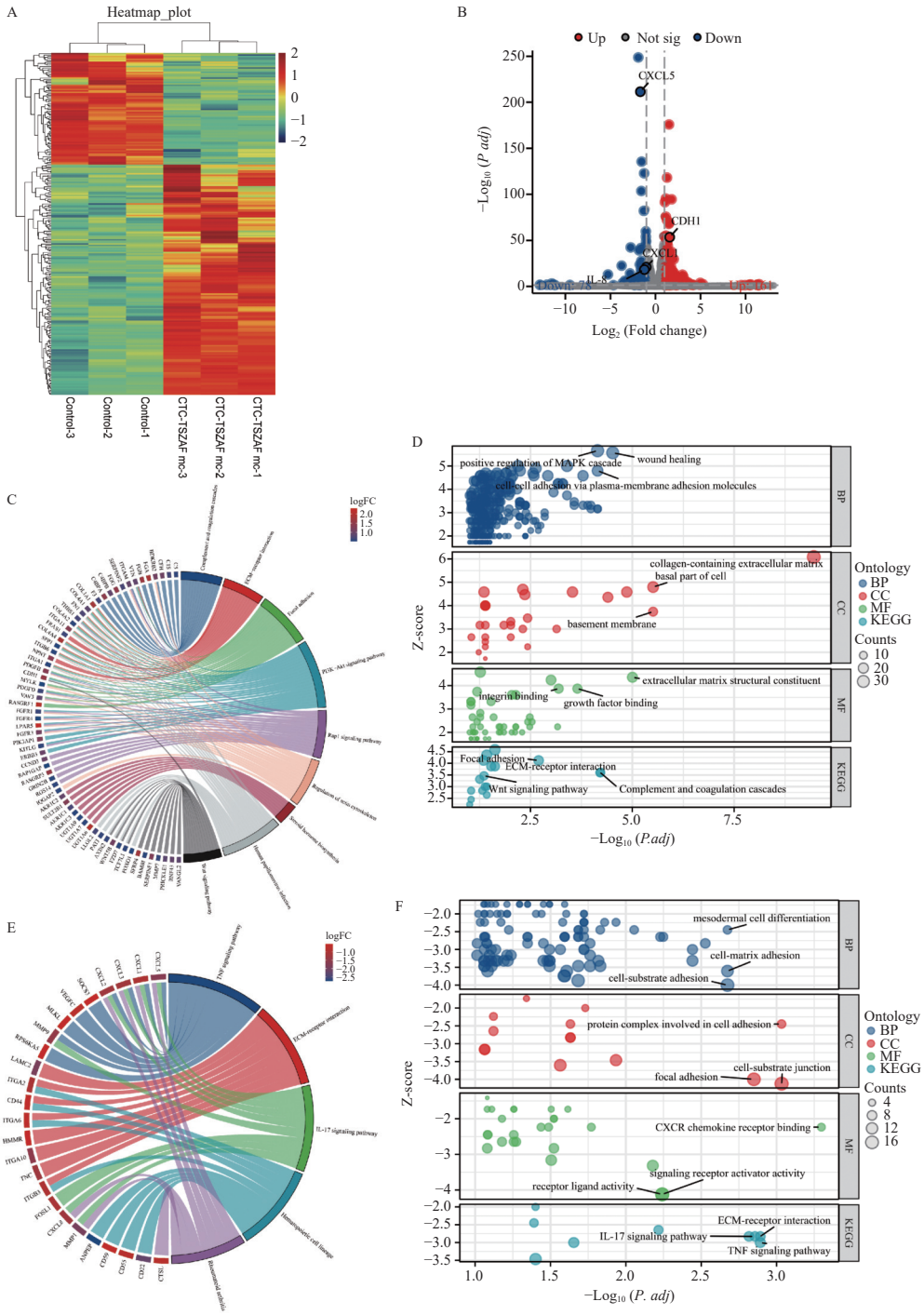

Fig. 5 RNA-Seq analysis of TSZAF mc treated CTC-TJH-01 cells. Heatmap plot (A) and Volcano plot (B) of differentially expressed genes between the TSZAF mc and control groups. GO and KEGG enrichment analysis of signaling pathways in biological processes (BP), cellular component (CC), and molecular function (MF) by (C and D) up and (E and F) down regulated genes, respectively.

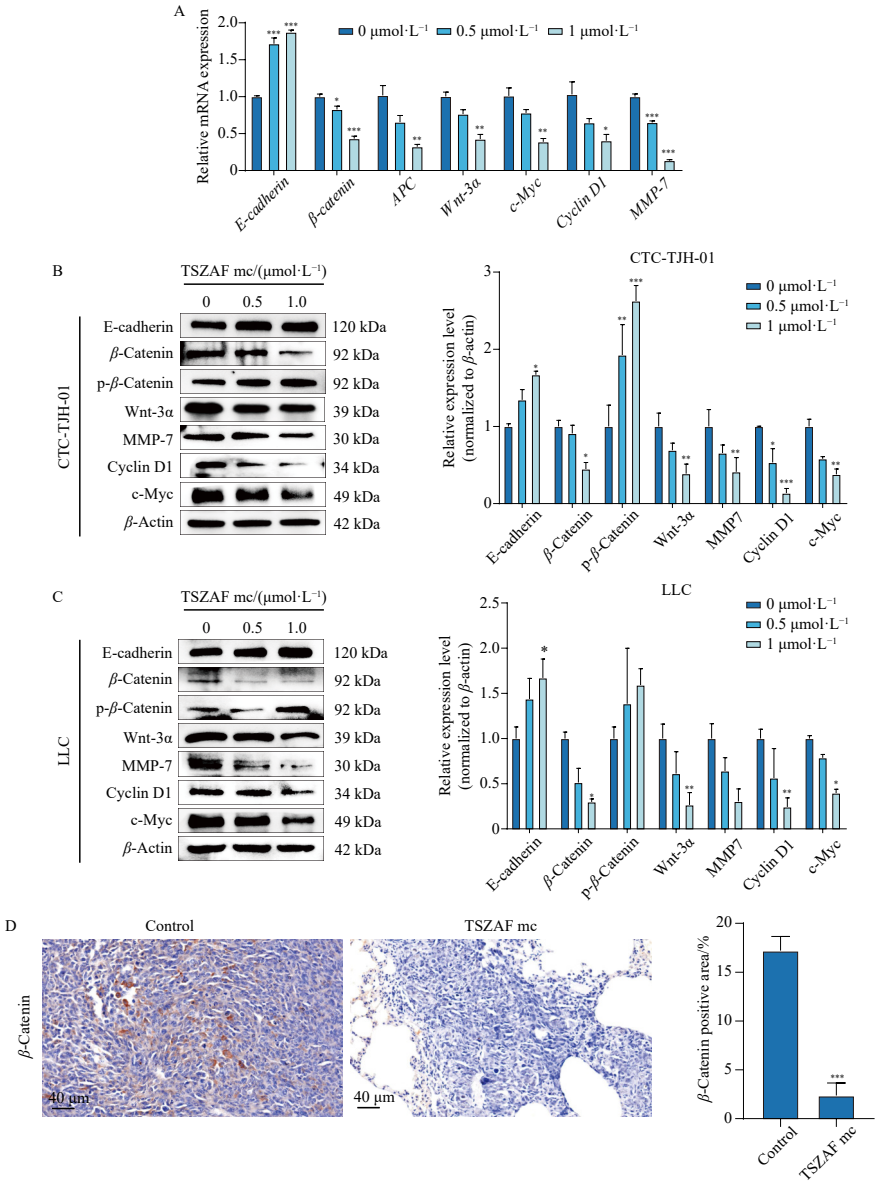

Fig. 6 TSZAF mc inhibited the Wnt/β-catenin signaling pathway in the lung cancer cells. (A) CTC-TJH-01 cells were treated with TSZAF mc (0, 0.5, 1 μmol·L^{-1}) for 24 h, then the relative mRNA expression levels of *E-cadherin*, *β-catenin*, *APC*, *Wnt-3α*, *c-Myc*, *Cyclin D1* and *MMP-7* were analyzed by RT-PCR. Each bar represents the mean ± SD of the three separate experiments. (B) The CTC-TJH-01 and (C) LLC cells were exposed to TSZAF mc (0, 0.5, 1 μmol·L^{-1}) for 24 h, the expression of E-cadherin, β-catenin, p-β-catenin, Wnt-3α, c-Myc, Cyclin D1 and MMP-7 was detected by WB. β-Actin was used as an internal standard. Each bar represents the mean ± SD of the three separate experiments. (D) The immunohistochemistry staining results of β-catenin expression in lung metastases. Each bar represents the mean ± SD (n = 8). $^{*}P < 0.05$, $^{**}P < 0.01$, $^{***}P < 0.001$ *vs* the control group.

mors shows positive correlation with prognosis [47]. Tumor cells recruit neutrophils into the tumor microenvironment by secreting chemokines, forming tumor-associated neutrophils (TANs) [48]. TANs contribute to tumor-promoted inflammation by facilitating angiogenesis, extracellular matrix remodeling, metastasis, and immunosuppression [49]. These findings suggest a potential association between the Wnt pathway and neutrophil-associated chemokine expression. Research indicates that inhibition of the

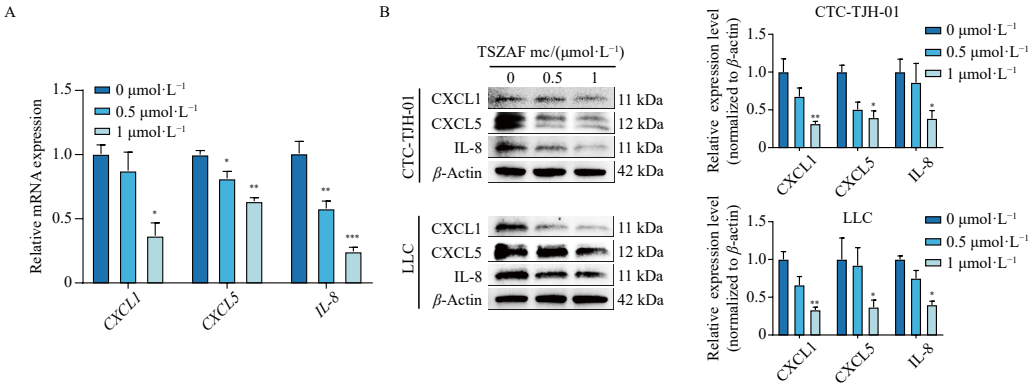

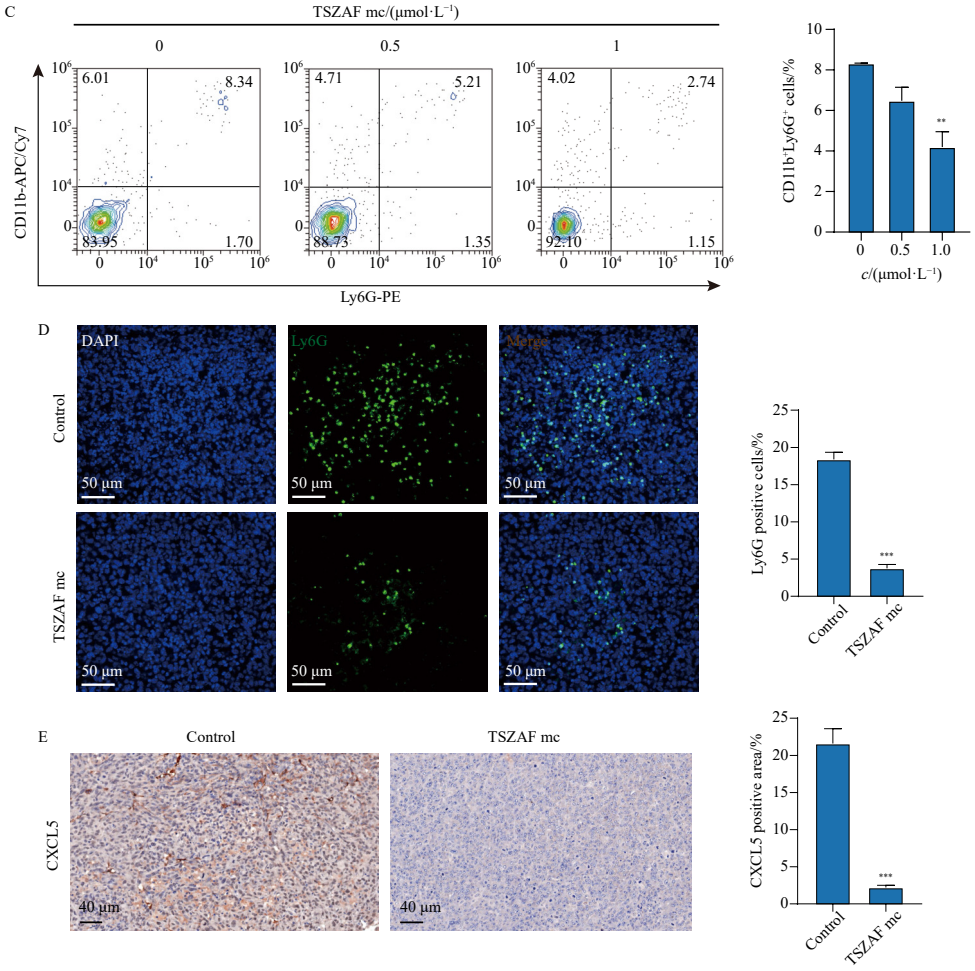

Fig. 7 TSZAF mc decreased the secretion of CXCL5 from tumor cells to reduce neutrophils infiltration. (A) CTC-TJH-01 cells was treated with TSZAF mc (0, 0.5, 1 μmol·L^{-1}) for 24 h, the relative mRNA expression levels of *CXCL1*, *CXCL5* and *IL-8* was analyzed by RT-PCR. Each bar represents the mean ± SD of the three separate experiments. (B) The CTC-TJH-01 and LLC cells were exposed to TSZAF mc (0, 0.5, 1 μmol·L^{-1}) for 24 h, the protein expression of CXCL1, CXCL5 and IL-8 were detected by WB. *β*-Actin was used as an internal standard. Each bar represents the mean ± SD of the three separate experiments. (C) The proportion of neutrophils recruited by LLC cells *in vitro* was detected by flow cytometry. Each bar represents the mean ± SD of the three separate experiments. (D) The IF staining results of Ly6G expression in lung metastases. Scale bar 50 μm. (E) The immunohistochemistry staining results of CXCL5 expression in lung metastases. Scale bar 40 μm. Each bar represents the mean ± SD (n = 8). $^{*}P < 0.05$, $^{**}P < 0.01$, $^{***}P < 0.001$ *vs* the control group.

Wnt signaling pathway reduces related chemokine expression [50]. However, the precise mechanism through which the Wnt pathway regulates chemokine expression remains undefined and requires additional investigation and validation.

In summary, this study identified TSZAF mc, a traditional Chinese medicine compound that effectively inhibits lung cancer metastasis and invasion. Mechanistically, TSZAF mc inhibited the proliferation, invasive and metastatic abilities of CTC-TJH-01 and LLC cells through down-regulation of the Wnt/*β*-catenin pathway and induction of apoptosis in lung cancer cells. Additionally, TSZAF mc reduced neutrophil infiltration in lung metastases by decreasing chemokine secretion, particularly CXCL5. These findings suggest that TSZAF mc represents a potential individualized therapeutic approach for the prevention and treatment of lung cancer metastasis.

Acknowledgements

We thank Shanghai Biochip Co., Ltd. for bioinformatics assistance.

Funding

This work was sponsored by the National Natural Science Foundation of China (Nos. 81973517, 82174245, 82174017, and 82305069), Shanghai Shenkang Hospital Development Center's Second Round of "Three-Year Action Plan to Promote Clinical Skills and Clinical Innovation in Municipal Hospitals" Research Physician Innovation and Translational Ability Training Project (No. SHDC2023CRD01), Shanghai Institute of Traditional Chinese Medicine and Psychosomatic Diseases 2023 Open Research Project (No. SZB2023102), Science and Technology Development Program of Shanghai University of Traditional Chinese Medicine in 2023 (No. 23KFL096) and Traditional Chinese Medicine Science and Technology Development Project of Shanghai Medical Innovation & Development Foundation (No. WL-HBRC-2021001K).

Availability of supporting information

Supporting information for this work can be obtained by contacting the corresponding authors *via* E-mail.

Declaration of competing interest

These authors have no conflict of interest to declare.

References

1 Siegel RL, Giaquinto AN, Jemal A. Cancer statistics, 2024. *CA Cancer J Clin*. 2024;74(1):12-49. https://doi.org/10.3322/caac.21820.

2 Xia C, Dong X, Li H, et al. Cancer statistics in China and United States, 2022: profiles, trends, and determinants. *Chin Med J*. 2022;135(5):584-590. https://doi.org/10.1097/CM9.0000000000002108.
3 Feng R, Su Q, Huang X, et al. Cancer situation in China: what does the China cancer map indicate from the first national death survey to the latest cancer registration? *Cancer Commun (Lond)*. 2023;43(1):75-86. https://doi.org/10.1002/cac2.12393.
4 Salas S, Cottet V, Dossus L, et al. Nutritional factors during and after cancer: impacts on survival and quality of life. *Nutrients*. 2022;14(14):2958. https://doi.org/10.3390/nu14142958.
5 Deng Z, Wu S, Wang Y, et al. Circulating tumor cell isolation for cancer diagnosis and prognosis. *EBioMedicine*. 2022;83:104237. https://doi.org/10.1016/j.ebiom.2022.104237.
6 Pereira-Veiga T, Schneegans S, Pantel K, et al. Circulating tumor cell-blood cell crosstalk: biology and clinical relevance. *Cell Rep*. 2022;40(9):111298. https://doi.org/10.1016/j.celrep.2022.111298.
7 Sun Y, Li T, Ding L, *et al*. Platelet-mediated circulating tumor cell evasion from natural killer cell killing through immune checkpoint CD155-TIGIT. *Hepatology*. 2025;81(3):791-807. https://doi.org/10.1097/HEP.0000000000000934.
8 Chemi F, Rothwell DG, McGranahan N, et al. Pulmonary venous circulating tumor cell dissemination before tumor resection and disease relapse. *Nat Med*. 2019;25(10):1534-1539. https://doi.org/10.1038/s41591-019-0593-1.
9 Crist SB, Ghajar CM. When a house is not a home: a survey of antimetastatic niches and potential mechanisms of disseminated tumor cell suppression. *Annu Rev Pathol*. 2021;16:409-432. https://doi.org/10.1146/annurev-pathmechdis-012419-032647.
10 Adachi H, Ito H, Sawabata N. Circulating tumor cells and the non-touch isolation technique in surgery for non-small-cell lung cancer. *Cancers (Basel)*. 2022;14(6):1448. https://doi.org/10.3390/cancers14061448.
11 Li Z, Xu K, Tartarone A, et al. Circulating tumor cells can predict the prognosis of patients with non-small cell lung cancer after resection: a retrospective study. *Transl Lung Cancer Res*. 2021;10(2):995-1006. https://doi.org/10.21037/tlcr-21-149.
12 Bidard FC, Kiavue N, Jacot W, et al. Overall survival with circulating tumor cell count-driven choice of therapy in advanced breast cancer: a randomized trial. *J Clin Oncol*. 2024;42(4):383-389. https://doi.org/10.1200/JCO.23.00456.
13 Li Y, Sheng H, Ma F, et al. RNA m(6)A reader YTHDF2 facilitates lung adenocarcinoma cell proliferation and metastasis by targeting the AXIN1/Wnt/β-catenin signaling. *Cell Death Dis*. 2021;12(5):479. https://doi.org/10.1038/s41419-021-03763-z.
14 Xiang D, Gu M, Liu J, et al. m6A RNA methylation-mediated upregulation of HLF promotes intrahepatic cholangiocarcinoma progression by regulating the FZD4/β-catenin signaling pathway. *Cancer Lett*. 2023;560:216144. https://doi.org/10.1016/j.canlet.2023.216144.
15 Tang Y, Tian W, Zheng S, et al. Dissection of FOXO1-induced LYPLAL1-DT Impeding triple-negative breast cancer progression *via* mediating hnRNPK/β-catenin complex. *Research (Wash D C)*. 2023;6:0289. https://doi.org/10.34133/research.0289.
16 Liu J, Xiao Q, Xiao J, et al. Wnt/β-catenin signalling: function, biological mechanisms, and therapeutic opportunities. *Signal Transduct Target Ther*. 2022;7(1):3. https://doi.org/10.1038/s41392-021-00762-6.
17 Zhang Y, Wang X. Targeting the Wnt/β-catenin signaling pathway in cancer. *J Hematol Oncol*. 2020;13(1):165. https://doi.org/10.1186/s13045-020-00990-3.
18 Stewart DJ. Wnt signaling pathway in non-small cell lung cancer. *J Natl Cancer Inst*. 2014;106(1):djt356. https://doi.org/10.1093/jnci/djt356.
19 Yang F, Xu J, Li H, et al. FBXW2 suppresses migration and invasion of lung cancer cells *via* promoting β-catenin ubiquitylation and degradation. *Nat Commun*. 2019;10(1):1382. https://doi.org/10.1038/s41467-019-09289-5.
20 Yu F, Yu C, Li F, et al. Wnt/β-catenin signaling in cancers and targeted therapies. *Signal Transduct Target Ther*. 2021;6(1):307. https://doi.org/10.1038/s41392-021-00701-5.
21 Xiong S, Dong L, Cheng L. Neutrophils in cancer carcinogenesis and metastasis. *J Hematol Oncol*. 2021;14(1):173. https://doi.org/10.1186/s13045-021-01187-y.
22 Huang X, Nepovimova E, Adam V, et al. Neutrophils in Cancer immunotherapy: friends or foes? *Mol Cancer*. 2024;23(1):107. https://doi.org/10.1186/s12943-024-02004-z.
23 Sun D, Tan L, Chen Y, et al. CXCL5 impedes CD8(+) T cell immunity by upregulating PD-L1 expression in lung cancer via PXN/AKT signaling phosphorylation and neutrophil chemotaxis. *J Exp Clin Cancer Res*. 2024;43(1):202. https://doi.org/10.1186/s13046-024-03122-8.
24 Ren W, Liang P, Ma Y, et al. Research progress of traditional Chinese medicine against COVID-19. *Biomed Pharmacother*. 2021;137:111310. https://doi.org/10.1016/j.biopha.2021.111310.
25 Que Z, Luo B, Yu P, et al. Polyphyllin VII induces CTC anoikis to inhibit lung cancer metastasis through EGFR pathway regulation. *Int J Biol Sci*. 2023;19(16):5204-5217. https://doi.org/10.7150/ijbs.83682.
26 Wang Z, Wu W, Wang Z, et al. Ex vivo expansion of circulating lung tumor cells based on one-step microfluidics-based immunomagnetic isolation. *Analyst*. 2016;141(12):3621-3625. https://doi.org/10.1039/C5AN02554K.
27 Lyden D, Ghajar CM, Correia AL, et al. Metastasis. *Cancer Cell*. 2022;40(8):787-791. https://doi.org/10.1016/j.ccell.2022.07.010.
28 Gerstberger S, Jiang Q, Ganesh K. Metastasis. *Cell*. 2023;186(8):1564-1579. https://doi.org/10.1016/j.cell.2023.03.003.
29 Chen X, Zhou F, Li X, et al. Folate receptor-positive circulating tumor cell detected by LT-PCR-based method as a diagnostic biomarker for non-small-cell lung cancer. *J Thorac Oncol*. 2015;10(8):1163-1171. https://doi.org/10.1097/JTO.0000000000000606.
30 Jin F, Zhu L, Shao J, et al. Circulating tumour cells in patients with lung cancer universally indicate poor prognosis. *Eur Respir Rev*. 2022;31(166):220151. https://doi.org/10.1183/16000617.0151-2022.
31 Que Z, Luo B, Zhou Z, et al. Establishment and characterization of a patient-derived circulating lung tumor cell line *in vitro* and *in vivo*. *Cancer Cell Int*. 2019;19:21. https://doi.org/10.1186/s12935-019-0735-z.
32 Fan L, Li Y, Sun Y, et al. Paris saponin VII inhibits the migration and invasion in human A549 lung cancer cells. *Phytother Res*. 2015;29(9):1366-1372. https://doi.org/10.1002/ptr.5389.
33 Xiang YC, Shen J, Si Y, et al. Paris saponin VII, a direct activator of AMPK, induces autophagy and exhibits therapeutic potential in non-small-cell lung cancer. *Chin J Nat Med*. 2021;19(3):195-204. https://doi.org/10.1016/S1875-5364(21)60021-3.
34 Cheng X, Gu J, Zhang M, et al. Astragaloside IV inhibits migration and invasion in human lung cancer A549 cells *via* regulating PKC-*α*-ERK1/2-NF-*κ*B pathway. *Int Immunopharmacol*. 2014;23(1):304-313. https://doi.org/10.1016/j.intimp.2014.08.027.
35 Xu F, Cui WQ, Wei Y, et al. Astragaloside IV inhibits lung cancer progression and metastasis by modulating macrophage polarization through AMPK signaling. *J Exp Clin Cancer Res*. 2018;37(1):207. https://doi.org/10.1186/s13046-018-0878-0.
36 Wang W, Huang Q, Chen Y, et al. The novel FAT4 activator jujuboside A suppresses NSCLC tumorigenesis by activating HIPPO signaling and inhibiting YAP nuclear translocation. *Pharmacol Res*. 2021;170:105723. https://doi.org/10.1016/j.phrs.2021.105723.
37 Que Z, Zhou Z, Luo B, et al. Jingfukang induces anti-cancer activity through oxidative stress-mediated DNA damage in circulating human lung cancer cells. *BMC Complement Altern Med*. 2019;19(1):204. https://doi.org/10.1186/s12906-019-2601-x.
38 Que ZJ, Yang Y, Liu HT, et al. Jinfukang regulates integrin/Src pathway and anoikis mediating circulating lung cancer cells migration. *J Ethnopharmacol*. 2021;267:113473. https://doi.org/10.1016/j.jep.2020.113473.
39 Que ZJ, Yao JL, Zhou ZY, et al. Jinfukang inhibits lung cancer metastasis by upregulating CX3CL1 to recruit NK cells to kill CTCs. *J Ethnopharmacol*. 2021;275:114175. https://doi.org/10.1016/j.jep.2021.114175.
40 Yang S, Liu Y, Li MY, et al. FOXP3 promotes tumor growth and metastasis by activating Wnt/β-catenin signaling pathway and EMT in non-small cell lung cancer. *Mol Cancer*. 2017;16(1):124. https://doi.org/10.1186/s12943-017-0700-1.
41 Sarode P, Zheng X, Giotopoulou GA, et al. Reprogramming of tumor-associated macrophages by targeting β-catenin/FOSL2/ARID5A signaling: A potential treatment of lung cancer. *Sci Adv*. 2020;6(23):eaaz6105. https://doi.org/10.1126/sciadv.aaz6105.
42 Liu Y, Lv H, Liu X, et al. The RP11-417E7.1/THBS2 signaling pathway promotes colorectal cancer metastasis by activating the Wnt/β-catenin pathway and facilitating exosome-mediated M2 macrophage polarization. *J Exp Clin Cancer Res*. 2024;43(1):195. https://doi.org/10.1186/s13046-024-03107-7.
43 Leppänen N, Kaljunen H, Takala E, et al. SIX2 promotes cell plasticity *via* Wnt/β-catenin signalling in androgen receptor independent prostate cancer. *Nucleic Acids Res*. 2024;52(10):5610-5623. https://doi.org/10.1093/nar/gkae206.
44 Muto S, Enta A, Maruya Y, et al. Wnt/β-catenin signaling and resistance to immune checkpoint inhibitors: from non-small-cell lung cancer to other cancers. *Biomedicines*. 2023;11(1):190. https://doi.org/10.3390/biomedicines11010190.
45 Guan S, Chen X, Chen Y, et al. FOXM1 variant contributes to gefitinib resistance *via* activating Wnt/β-catenin signal pathway in patients with non-small cell lung cancer. *Clin Cancer Res*. 2022;28(17):3770-3784. https://doi.org/10.1158/1078-0432.CCR-22-0791.
46 Szczerba BM, Castro-Giner F, Vetter M, et al. Neutrophils escort circulating tumour cells to enable cell cycle progression. *Nature*. 2019;566(7745):553-557. https://doi.org/10.1038/s41586-019-0915-y.
47 Gungabeesoon J, Gort-Freitas NA, Kiss M, et al. A neutrophil response linked to tumor control in immunotherapy. *Cell*. 2023;186(7):1448-1464. e1420. https://doi.org/10.1016/j.cell.2023.02.032.
48 Gentles AJ, Newman AM, Liu CL, et al. The prognostic landscape of genes and infiltrating immune cells across human cancers. *Nat Med*. 2015;21(8):938-945. https://doi.org/10.1038/nm.3909.
49 Jaillon S, Ponzetta A, Di Mitri D, et al. Neutrophil diversity and plasticity in tumour progression and therapy. *Nat Rev Cancer*. 2020;20(9):485-503. https://doi.org/10.1038/s41568-020-0281-y.
50 Milosevic V, Kopecka J, Salaroglio IC, et al. Wnt/IL-1β/IL-8 autocrine circuitries control chemoresistance in mesothelioma initiating cells by inducing ABCB5. *Int J Cancer*. 2020;146(1):192-207. https://doi.org/10.1002/ijc.32419.